Operation and Design Optimization of Microgrids With Renewables

Bing Yan, *Member, IEEE*, Peter B. Luh, *Fellow, IEEE*, Guy Warner, and Peng Zhang, *Senior Member, IEEE*

***Abstract*— To reduce energy costs and emissions of microgrids, daily operation is critical. The problem is to commit and dispatch distributed devices with renewable generation to minimize the total energy and emission cost while meeting the forecasted energy demand. The problem is challenging because of the intermittent nature of renewables. In this paper, photovoltaic (PV) uncertainties are modeled by a Markovian process. For effective coordination, other devices are modeled as Markov processes with states depending on PV states. The entire problem is Markovian. This combinatorial problem is solved using branch-and-cut. Beyond energy and emission costs, to consider capital and maintenance costs in the long run, microgrid design is also essential. The problem is to decide device sizes with given types to minimize the lifetime cost while meeting energy demand. Its complexity increases exponentially with the problem size. To evaluate the lifetime cost including the reliability cost and the classic components such as capital and fuel costs, a linear model is established. By selecting a limited number of possible combinations of device sizes, exhaustive search is used to find the optimized design. The results show that the operation method is efficient in saving cost and scalable, and microgrids have lower lifetime costs than conventional energy systems. Implications for regulators and distribution utilities are also discussed.**

***Note to Practitioners*—In a microgrid, e.g., for a school campus or a residential community, a set of distributed energy devices generate and store different types of energy such as electricity and steam to meet time-varying electricity and thermal demand. They should be coordinated through daily operation to reduce energy costs and greenhouse gas emissions. In this paper, a novel model is established for operation to reduce daily energy and CO_2 emission costs. By solving the problem, optimized operation strategies are obtained. To consider capital and maintenance costs in the long run, microgrid design is also critical. To evaluate the lifetime cost including the reliability cost and the classic components such as capital and fuel costs, a linear model is established. By exhaustively searching through the limited number of selected combinations of device sizes, the optimized design is found. The results show that the total energy and emission cost is reduced by the optimized operation compared with the selected heuristic operation, and microgrids have lower lifetime costs than conventional energy systems. Implications for regulators and distribution utilities are also discussed.**

***Index Terms*— Branch-and-cut, design, emissions, microgrids, operation.**

Manuscript received August 18, 2016; revised October 26, 2016; accepted November 25, 2016. Date of publication February 20, 2017; date of current version April 5, 2017. This paper was recommended for publication by Associate Editor J. Li and Editor S. Grammatico upon evaluation of the reviewers' comments. This work was supported by Pareto Energy, Ltd. The views expressed in this paper are solely those of the authors and do not necessarily represent those of Pareto Energy Ltd.

B. Yan, P. B. Luh, and P. Zhang are with the Department of Electrical and Computer Engineering, University of Connecticut, Storrs, CT 06269 USA (e-mail: bing.yan@uconn.edu).

G. Warner is with Pareto Energy, Ltd., Washington, DC 20037 USA (e-mail: gwarner@paretoenergy.com).

This paper has supplementary downloadable multimedia material available at http://ieeexplore.ieee.org provided by the authors. The Supplementary Material contains a presentation of the paper. This material is 948 KB in size.

Color versions of one or more of the figures in this paper are available online at http://ieeexplore.ieee.org.

Digital Object Identifier 10.1109/TASE.2016.2645761

I. Introduction

With the world's increasing energy demand and growing environmental concerns, efficient utilization of energy is essential for sustainable living, especially renewable energy. Flexible and reliable microgrids, which can operate under the grid-connected mode and can also turn into an islanded mode [1], [2], provide a promising opportunity and a desirable infrastructure. In microgrids, different distributed energy devices, such as gas turbines (GTs), photovoltaic (PV) panels, and natural gas boilers, generate and store different types of energy such as electricity, steam, and hot/chilled water to satisfy time-varying electricity and thermal demand. They should be coordinated through daily operation to reduce the energy costs and greenhouse gas emissions. To consider capital and maintenance costs in the long run, microgrid design (device types and sizes) is also critical.

The microgrid under consideration involves different distributed energy devices: combined cooling heat and power (CCHP), PV panels, natural gas boilers, electrical chillers, and batteries, chosen among commonly used devices in practical microgrids. The microgrid operation problem is hierarchical from unit commitment to economic dispatch to optimal power flow. Focusing on the first two, the problem under consideration is to commit and dispatch distributed devices to minimize energy and CO_2 emission costs under the grid-connected mode while meeting hourly day-ahead electricity and thermal demand. The islanded mode and the transition between the two modes are not considered since they are not economics. The design problem is to decide device sizes with given types and the type of grid-connection to minimize the lifetime cost while satisfying energy demand.

Optimized microgrid operation, however, is challenging because of the intermittent nature of renewables. In the literature, uncertainties were usually modeled by scenarios in microgrid operation problems. However, it is difficult to select an appropriate number of scenarios to balance modeling accuracy, computational efficiency, and solution feasibility. In this paper, a mixed-integer model is established from the energy and emission point of view in Section III. To avoid the difficulties associated with scenario-based methods, our idea is to model PV generation by a Markovian process with the current state summarizing all the past information. For

effective coordination, other devices are modeled as Markov processes correspondingly with states depending on PV states. The entire problem is therefore Markovian. This combinatorial problem is solved using branch-and-cut.

Optimized design is also challenging since the problem complexity increases exponentially as the problem size increases, and energy resources (e.g., solar irradiance), fuel prices, and load are uncertain. In addition, the reliability costs, i.e., costs of protection devices and costs of unserved load when there is no power supply, need to be considered. In the literature, software packages were used, with uncertainties addressed by sensitivity analysis, while reliability costs were rarely considered. In this paper, a linear model is established in Section IV to evaluate the microgrid lifetime cost including the reliability cost and the classic components such as capital and fuel costs. The modeling of daily operation is simplified since it is consistent with that in the operation problem. The reliability cost is obtained based on the microgrid configuration and the estimated cost of unserved load during power outages. Based on load profiles, a limited number of possible combinations of device sizes are considered. With heuristic strategies for daily operation, exhaustive search is used to find the optimized design.

In Section V, two examples are presented. The first small example is to illustrate the Markov-based modeling of PV generation in operation and show different components of the lifetime cost in design. The second semirealistic one is to show that the operation method is efficient in saving cost and scalable. It is also to compare lifetime costs of different design configurations and show impacts of uncertain factors in the design. The implications of the above models and methods on the microgrid operation and design for regulators and distribution utilities are discussed in Section VI.

II. Literature Review

To formulate and solve the microgrid operation problem, models and methods provided in the literature are reviewed in Section II-A. Related works on microgrid design are reviewed in Section II-B. Our earlier work is briefly reviewed in Section II-C. Since operation and design problems of distributed energy systems (DESs) are similar to those of microgrids, related studies are also involved.

A. Operation of Microgrids

The microgrid operation problem is hierarchical from unit commitment to economic dispatch to optimal power flow. Many researchers focus on unit commitment and economic dispatch of microgrids or DESs in the literature. Some of them focus on reducing energy costs as the single objective through daily operation [3]–[11]. For example, a mixed-integer linear model was developed to minimize the daily energy costs of grid power and natural gas for a microgrid while satisfying energy demand [3]. In this model, PV generation was modeled by a deterministic approach without explicitly considering uncertainties, calculated offline with the given parameters and solar irradiation. The battery was modeled by standard dynamics for state of charge without energy losses. The electrical grid was simplified by modeling electricity balance, i.e., electricity generated by the microgrid and bought from the grid equals electricity consumed in the microgrid, where the detailed electrical power models were not considered. The problem was solved using branch-and-cut and the impacts of uncertain demand and renewable generation were analyzed by the scenario tree method. In [4], a mixed-integer nonlinear model was developed, where PV and wind uncertainties were modeled by scenarios. It is, however, difficult to select an appropriate scenario number to balance modeling accuracy, computational efficiency, and solution feasibility. Batteries were modeled by standard state dynamics considering charge and discharge efficiencies, and the electrical grid was simplified by modeling electricity balance. A metaheuristic algorithm was used to solve the problem. A decentralized energy management system was developed by Siemens for virtual power plants to minimize overall costs through coordination of distributed generators and energy storage [5]. With simplified energy device models, the modeling of renewable generation is based on forecasting and the overall problem is not stochastic.

Beyond considering energy costs as a single objective, multiobjective optimization methods were also developed for microgrid or DES operation by taking other factors such as emissions into account [12], [13]. In [12], a stochastic model was developed to minimize costs and emissions, with demand and renewable generation uncertainties modeled by scenarios. A teaching-learning-based optimization algorithm was developed to solve the problem. In [14], a deterministic model was developed to minimize the power generation cost and to maximize the useful life of batteries without considering renewable generation uncertainties. The problem was solved by a genetic algorithm, and testing was carried out using the actual measured data.

B. Design of Microgrids

In the microgrid/DES operation problem, device types and sizes are given, while capital and maintenance costs are not considered. In the long run, determining device types and sizes is also critical. In the literature, mathematical models and optimization methods were developed for optimal design of microgrids or DESs to minimize the total annual cost or lifetime cost [15]–[24]. Since the design horizon is much longer than the operation one, the uncertainties of renewable generation will be averaged out and are usually not considered in the design problem. In addition, reliability costs were rarely considered within the design framework.

In the design problem, the daily operation strategies were usually considered for four typical season days, and each day repeats for the entire season [15]–[19]. To select optimal device sizes based on given types (with constant efficiencies), a linear model was developed to minimize the annual cost of a microgrid [15]. The formulation was deterministic, and wind uncertainties were modelled by repeatedly running the deterministic model in a Monte Carlo simulation. The problem was solved by the simplex method. To decide both device types and sizes (with constant efficiencies), a mixed-integer linear problem was developed in [16]. The problem was solved using branch-and-bound combined with the simplex method. Since the energy demand, electricity and gas prices, and the carbon

tax rate are uncertain, sensitivity analysis was executed on those factors. To consider the varying device efficiencies with generation levels, a more complex mixed-integer nonlinear model was presented in [17]. Given the nonlinear nature caused by varying efficiencies, after convex underestimation and linearization by introducing new variables, the problem was solved using branch-and-bound for near-optimal solutions.

In some studies, daily operation strategies were considered for more than four days in a year. For simplicity, heuristic operation strategies were used, where operation optimization was not involved [19]–[24]. To minimize total lifetime costs, exhaustive search was used to find the optimal design with a limited number of possible combinations of device types and sizes in [19]–[22]. Sensitivity analysis was used to explore the impacts of uncertain factors such as load and fuel prices. With the consideration of multiple objectives, the genetic algorithm was used to find the optimal design of microgrids and DESs (without considering thermal energy) in [23] and [24]. In [23], a hybrid PV–wind–diesel microgrid with batteries was considered, a multiobjective model was established to minimize the lifetime cost and emissions. Sensitivity analysis was conducted for inflation of diesel fuel prices, acquisition costs of PV panels, and emissions from PV panels. In [24], a similar model was devolved to minimize lifetime costs, CO_2 emissions, and unmet load simultaneously, and the problem was also solved by the same method.

C. Our Previous Work

To overcome the difficulties caused by scenario-based methods, a Markovian approach was developed to solve day-ahead unit commitment problems in [25]. Without considering transmission capacities, wind generation was aggregated and modeled as a Markov chain, where a state represents the wind generation at a particular hour, capturing all the past information. Since the number of states increases linearly with that of hours, the complexity is significantly reduced compared with scenario-based methods. A detailed complexity comparison among the deterministic approach, stochastic programming, and our approach can be found in [25, Sec. V-D]. Testing results demonstrate the computational efficiency, the effectiveness to accommodate high-level wind penetration, and the ability to capture low-probability high-impact events of our approach. The approach thus represents a new and effective way to address stochastic problems without scenario analysis.

Recently, we also established a mixed-integer linear model for operation optimization of DESs (without batteries) to minimize the energy cost and increase the total exergy efficiency of a DES [26]. Without considering renewable uncertainties, the deterministic problem was solved using branch-and-cut. To reduce the energy cost and CO_2 emissions, a similar model was developed in [27] and the problem was solved by the same method. In [28], a more complicated mixed-integer model was developed to reduce the energy cost and exergy losses at the energy conversion step, which accounts for the largest part of the total exergy loss in the whole energy supply chain. The surrogate Lagrangian relaxation method was used to solve the problem. In these three papers, uncertainties of renewable generation were not taken into account.

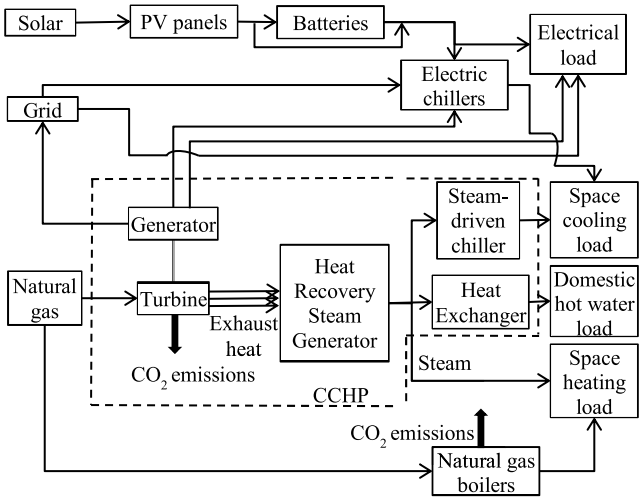

Fig. 1. Configuration of the microgrid under consideration.

III. Operation Problem

In this section, the operation problem is described in Section III-A. The mathematical formulation is established in Section III-B. Based on the problem characteristics, the solution methodology is briefly presented in Section III-C.

A. Problem Description

For operation, the microgrid under consideration involves different distributed energy devices as shown in Fig. 1. The CCHP system consists of multiple GTs and heat recovery steam generators, a steam-driven absorption chiller, and a heat exchanger, as sketched inside by the dashed lines. Electrical load and electricity required by electric chillers can be satisfied by the grid power, CCHP, PV panels, and batteries. The microgrid can also sell extra electricity back to the grid. The electric and steam-driven chillers are used for space cooling, while steam and natural gas boilers for space heating. The domestic hot water load can be met by steam through the heat exchanger with sufficient exhaust heat from power generation. From the environmental point of view, combustion of natural gas in the CCHP and boilers causes CO_2 emissions.

Consider the daily operation of a microgrid over 24 (T) h with each hour indexed by t ($1 \leq t \leq T$). For devices, their properties such as cost functions and capacities are assumed known. Energy demand including electricity, space heating/cooling, and domestic hot water is also assumed known at hour t. The operation problem is to decide the device operation strategies such as ON/OFF statuses and generation levels to reduce the total energy and emission cost while meeting the given time-varying demand and satisfying individual device constraints.

B. Problem Formulation

For microgrid operation under the grid-connected mode, a mixed-integer model is established from the energy and emission point of view. The modeling of devices is presented in Section III-B1, and the focus is on PV generation since the intermittent nature of renewables is a major challenge in

modeling. System balance is formulated in Section III-B2. The objective function is discussed in Section III-B3.

1) Modeling of Devices: As mentioned earlier, this paper is on unit commitment and economic dispatch, and device modeling focuses on ON/OFF statuses and generation levels as in [3]–[9]. For simplicity, device efficiencies are assumed constant, although they generally depend on generation levels. This fixed-efficiency assumption has often been used in the literature for microgrid design and operation optimization to maintain problem linearity [3], [15]. The modeling of the CCHP, boilers, chillers, PV, and battery is presented as follows, and constraints generally include capacity, energy consumption, and emissions.

a) Modeling of CCHP [29]: In the CCHP, GTs are used to meet electrical load by natural gas, while the fossil fuel combustion causes emissions. Then, exhaust heat is recovered in heat recovery steam generators, and the high-temperature steam could be directly used for space heating or sent to the absorption chiller and heat exchanger for space cooling and domestic hot water, respectively. Constraints for the CCHP are presented as follows.

Capacity constraints of GTs: The generation level of the mth GT $P_m^{\mathrm{GT}}(t)$ (continuous decision) should be within its minimum $P_m^{\mathrm{GT,min}}$ and maximum $P_m^{\mathrm{GT,max}}$ if the device is ON [ON/OFF binary decision $x_m^{\mathrm{GT}}(t) = 1$], that is

$$P_m^{\mathrm{GT,min}}\, x_m^{\mathrm{GT}}(t) \le P_m^{\mathrm{GT}}(t) \le P_m^{\mathrm{GT,\,max}}\, x_m^{\mathrm{GT}}(t). \tag{1}$$

For other devices, this constraint is omitted.

Gas consumption of GTs: The amount of natural gas needed in the mth GT $G_m^{\mathrm{GT}}(t)$ is calculated as follows:

$$G_m^{\mathrm{GT}}(t) = P_m^{\mathrm{GT}}(t)/(\eta^{e,\mathrm{GT}} HV^{\mathrm{Gas}}), \tag{2}$$

where $\eta^{e,\mathrm{GT}}$ is the gas-to-electric efficiency and HV^{gas} is the heat value of natural gas.

CO_2 emissions of GTs: The amount of CO_2 due to the natural gas combustion in the mth GT $Env_m^{\mathrm{GT}}(t)$ is

$$Env_m^{\mathrm{GT}}(t) = G_m^{\mathrm{GT}}(t) HV^{\mathrm{Gas}} G^{cin}, \tag{3}$$

where G^{cin} denotes the carbon intensity of natural gas.

Heat of exhaust gas in turbines: The amount of heat contained in the exhaust gas from the mth GT $Q_m^{\mathrm{GT}}(t)$ is

$$Q_m^{\mathrm{GT}}(t) = P_m^{\mathrm{GT}}(t)\eta^{th,\mathrm{GT}}/\eta^{e,\mathrm{GT}}, \tag{4}$$

where $\eta^{th,\mathrm{GT}}$ is the thermal efficiency of the GT.

Total steam: Steam generated by all steam generators could be directly used for space heating $Q^{\mathrm{Steam-SH}}(t)$, sent to the absorption chiller for space cooling $Q^{\mathrm{Steam-SC}}(t)$ or sent to the heat exchanger for domestic hot water $Q^{\mathrm{Steam-DHW}}(t)$, that is

$$\sum_m Q_m^{\mathrm{GT}}(t)\eta^{HRSG} = Q^{\mathrm{Steam-SH}}(t) + Q^{\mathrm{Steam-SC}}(t) + Q^{\mathrm{Steam-DHW}}(t), \tag{5}$$

where η^{HRSG} is the energy efficiency of the steam generator.

Heat in the heat exchanger: The amount of heat provided by the heat exchanger for domestic hot water $H^{\mathrm{HE\text{-}DHW}}(t)$ is

$$H^{\mathrm{HE\text{-}DHW}}(t) = Q^{\mathrm{Steam\text{-}DHW}}(t)\eta^{\mathrm{HE}}, \tag{6}$$

where η^{HE} is the efficiency of the heat exchanger.

Cooling in the absorption chiller: The amount of cooling provided by the absorption chiller $C^{\mathrm{SChiller}}(t)$ is

$$C^{\mathrm{SChiller}}(t) = Q^{\mathrm{Steam-SC}}(t)\eta^{\mathrm{HR,SChiller}} COP^{\mathrm{SChiller}}, \tag{7}$$

where $\eta^{\mathrm{HR,SChiller}}$ and COP^{SChiller} denote the heat recovery efficiency and coefficient of performance of the chiller, respectively.

b) Modeling of natural gas boilers:

Gas consumption of boilers: The amount of gas needed in the nth natural gas boiler $G_n^{\mathrm{boiler}}(t)$ is calculated as follows:

$$G_n^{\mathrm{boiler}}(t) = H_n^{\mathrm{boiler}}(t)/(\eta^{\mathrm{boiler}} HV^{\mathrm{Gas}}), \tag{8}$$

where $H_n^{\mathrm{boiler}}(t)$ denotes the heat generation level of the boiler and η^{boiler} is the efficiency of the boiler. The modeling of CO_2 emissions $Env_n^{\mathrm{boiler}}(t)$ is similar to that of GTs.

c) Modeling of electric chillers:

Electricity consumption of electric chillers: The electricity required by the lth electric chiller $P_l^{\mathrm{EChiller}}(t)$ is

$$P_l^{\mathrm{EChiller}}(t) = C_l^{\mathrm{EChiller}}(t)/(\eta^{\mathrm{EChiller}} COP^{\mathrm{EChiller}}), \tag{9}$$

where $C_l^{\mathrm{EChiller}}(t)$ denotes the amount of cooling generated in the electric chiller and η^{EChiller} and COP^{EChiller} denote the efficiency and coefficient of performance of the chiller, respectively.

d) Modeling of PV generation: Ideally, the PV generation behaves like a sinusoidal wave with zero values for darkness hours [30], [31]. The amplitude and frequency of the sinusoidal wave depend on the PV capacities and locations, and seasons. PV generation can change significantly depending on weather conditions such as clouds. The PV generation therefore depends on ideal generation and uncertain weather conditions. To avoid the computational complexity caused by scenario-based methods as discussed in Section II, a Markov-based model is established to integrate intermittent and uncertain PV generation into microgrids based on our early work for wind [25]. In the model, weather uncertainties are assumed to be a Markovian process with N states (as a percentage of the ideal weather conditions) and state i is denoted by W_i, following related real case studies in [32] and [33].

Based on historical data, the probability that the current weather state is j if the previous state was i can be obtained as follows [34]:

$$P_{ij} = \frac{\text{observed transitions from state } i \text{ to } j}{\text{ocurrencesof state } i}. \tag{10}$$

In this way, the state transition matrix P^{ST} can be established. To solve the problem for a specific region, the historical data should be analyzed to determine the number of states to balance modeling accuracy and computation efficiency. The transition matrix should be also updated by incorporating the latest weather forecast. Because of seasonal behaviors, for each season, a transition matrix is needed.

With weather conditions modeled about, the uncertain PV generation $P_i^{\mathrm{PV}}(t)$ is also a Markovian process as follows:

$$P_i^{\mathrm{PV}}(t) = P^{\mathrm{IPV}}(t)\, W_i, \tag{11}$$

where $P^{\mathrm{IPV}}(t)$ is the ideal PV generation. The probability that the PV generation is $P_i^{\mathrm{PV}}(t)$ at time t, denoted by $\phi_i(t)$, is the

sum of the probabilities at time $t-1$ weighted by different transitions

$$\varphi_i(t) = \sum_{j=1}^{N} P_{ji}\varphi_j(t-1). \tag{12}$$

The probabilities of PV generation levels for future time slots can be obtained based on the initial PV generation state and the transition matrix.

e) Modeling of battery: To capture state dynamics, a simplified battery model is used here, assuming that charging/discharging efficiencies are 100%. The battery charge and discharge are extended to depend on PV states. The state of charge at time t under PV state i is denoted by $P_i^{Bat}(t)$. The standard 1-D state equation on state of change in the literature is extended to 2-D on state of change and PV states as follows:

$$P_i^{\mathrm{Bat}}(t+1) = P_j^{\mathrm{Bat}}(t) + P_i^{\mathrm{bc}}(t) - P_i^{\mathrm{bd}}(t) \quad \forall j, \quad \forall i \in \{i|\varphi_i(t) \neq 0\}. \tag{13}$$

In addition, it cannot be charged and discharged simultaneously.

f) Modeling of CCHP, boilers, and chillers based on PV states: For effective coordination, other devices are modeled as Markov processes correspondingly with states depending on the states of PV generation. The generation levels of CCHP, boilers, and electric chillers, and the amount of grid power (electricity from or to the grid) are therefore modeled to depend on PV states. Take the mth GT in CCHP as an example. For each PV state i, there is a corresponding generation level $P_{m,i}^{\mathrm{GT}}(t)$ (continuous decision). The other devices are modeled in a similar way.

2) Modeling of System Balance: The modeling of electrical grid is simplified by modeling electricity balance as in [3]–[9], where detailed electrical power models are not considered.

a) Electricity balance: In the microgrid, the summation of electricity generated by PV panels and the CCHP, discharged by the battery, and bought from the grid equals the summation of electricity demand and electricity consumed by electric chillers, sold to the grid, and stored. The electricity balance constraint should be satisfied at every hour for each PV state where its probability is nonzero, that is

$$P_i^{\mathrm{PV}}(t) + \sum_m P_{m,i}^{\mathrm{GT}}(t) + P_i^{\mathrm{bd}}(t) + P_i^{\mathrm{buy}}(t) = P^{\mathrm{dem}}(t) + \sum_l P_{l,i}^{\mathrm{EChiller}}(t) + P_i^{\mathrm{sell}}(t) + P_i^{\mathrm{bc}}(t) \quad \forall i \in \{i|\varphi_i(t) \neq 0\}. \tag{14}$$

New decision variables are $P_i^{\mathrm{buy}}(t)$ and $P_i^{\mathrm{sell}}(t)$, the amount of electricity bought from and sold to the grid, respectively. The demand $P^{\mathrm{dem}}(t)$ is assumed given, not varying with PV states.

b) Thermal balance: For space heating, the summation of heat generated by natural gas boilers and provided by steam equals the demand $P^{\text{dem-SH}}(t)$, that is

$$\sum_n H_{n,i}^{\mathrm{boiler}}(t) + Q_i^{\mathrm{Steam-SH}}(t) = H^{\mathrm{dem-SH}}(t) \quad \forall i \in \{i|\varphi_i(t) \neq 0\}. \tag{15}$$

The thermal balance for space cooling and domestic hot water is formulated in a similar way.

The entire problem is therefore Markovian.

3) Objective Function: The objective is to minimize the total daily cost, i.e., energy and emission costs. The energy cost *Cost* consists of three terms, buying natural gas from the station and electricity from the grid and selling electricity back to the grid, that is

$$Cost = \sum_t \sum_i \varphi_i(t)\left(C^{\mathrm{Gas}} \times \left(\sum_m G_{m,i}^{\mathrm{GT}}(t) + \sum_n G_{n,i}^{\mathrm{boiler}}(t)\right) + C^{\mathrm{Grid,buy}}(t) \times P_i^{\mathrm{buy}}(t) - C^{\mathrm{Grid,sell}}(t) \times P_i^{\mathrm{sell}}(t)\right) \cdot \Delta t, \tag{16}$$

where $C^{\mathrm{Grid,buy}}(t)$ and $C^{\mathrm{Grid,sell}}(t)$ denote the unit price of electricity from and to the grid at time t, respectively; C^{Gas} is the unit price of natural gas; and Δt is the time slot length.

To quantify the cost of CO_2 emissions caused by the natural gas combustion in GTs and boilers, the carbon tax *CarbonTax* is considered here (currently not for individual microgrids) [35], that is

$$CarbonTax = P^{\mathrm{CTax}} \sum_t \sum_i \varphi_i(t) \times \left(\sum_m Env_{m,i}^{\mathrm{GT}}(t) + \sum_n Env_{n,i}^{\mathrm{boiler}}(t)\right), \tag{17}$$

where P^{CTax} denotes the carbon tax on CO_2 emissions (\$/kg). Since the carbon tax associated with grid power generation is already reflected in the grid price, it is not involved here.

Based on the above, the overall objective to be minimized is *Cost* +*CarbonTax*.

4) Solution Methodology: The problem formulated above is stochastic and linear and involves both discrete and continuous variables. Branch-and-cut, which is powerful for mixed-integer linear problems, is therefore used. In the method, all integrality requirements on variables are first relaxed, and the relaxed problem can be efficiently solved using a linear programming method. The solution also provides a lower bound. If the values of all integer decision variables turn out to be integers, the solution is optimal to the original problem. If not, valid cuts that do not cut off feasible integer solutions are added, trying to obtain the convex hull. Once the convex hull is obtained, the values of all integer decision variables in the solution to the relaxed problem are integers, and this solution is optimal to the original problem. If the convex hull cannot be obtained by cuts, low-efficient branching operations are needed. Optimization stops when computational time reaches the preset stop time or the relative gap (relative difference between the objectives of the optimal relaxed solution and current integer solution) falls below the preset gap [36].

IV. Design Problem

In this section, the design problem is described in Section IV-A. The problem is formulated in Section IV-B. The solution methodology is presented in Section IV-C.

A. Problem Description

The above operation problem is to decide daily operation strategies of microgrids with fixed device types and sizes to reduce the total daily cost in the short run, while the design problem is to decide device sizes with the given types and the type of grid connection (synchronized or non-synchronized) to reduce the lifetime cost in the long run. The lifetime cost consists of the reliability cost and classic cost components including capital, replacement, operation and maintenance (O&M), fuel, and emission costs. The O&M, fuel, and emission costs are based on the daily operation of devices. For simplicity, four typical season days with heuristic operation strategies are considered, while operation optimization is not involved.

Consider the design problem for a microgrid over its entire lifetime, N years with each year indexed by t ($1 \le t \le N$). Devices include the CCHP, natural gas boilers, electrical chillers, PV panels, and batteries, where their properties such as capital costs, lifetimes, and efficiencies are assumed known. Electricity, space heating/cooling, and domestic hot water demand for four typical season days are assumed known.

B. Problem Formulation

Since the time horizon for design is much longer than that for operation, a linear model is established in this section. The modeling of devices is discussed in Section IV-B1. The focus is on the lifetime cost, and the modeling of daily operation is simplified since it is consistent with that in the operation problem. The system balance is briefly presented in Section IV-B2. The reliability cost is discussed in detail in Section IV-B3. The objective function is described in Section IV-B4.

1) Modeling of Devices: The device modeling includes four parts, i.e., costs, operation constraints, energy consumption, and emissions. The associated cost includes the capital, replacement, O&M, and fuel costs and carbon tax. Because the device lifetime may not be consistent with the microgrid lifetime, the salvage value, i.e., the remaining value at the end of the project lifetime, is also taken into account. The design problem is usually over 20 years, and therefore, discounting and inflation have to be considered. Based on the above, the net present cost (NPC) of a device is the present value of all the costs over the project lifetime minus its salvage value. Consider a GT in the CCHP as an example. For illustration purposes, it is assumed that the lifetime of the GT is longer than that of the microgrid, and there are no replacement costs. The NPC C_{GT}^{NPC} is calculated as follows:

$$C_{GT}^{\mathrm{NPC}} = C_{GT}^{\mathrm{Cap}} - C_{GT}^{\mathrm{Sal}}/(1+i)^N + \sum_{t=1}^{T}\left(C_{GT,t}^{\mathrm{O\,\&\,M}} + C_{GT,t}^{\mathrm{Fuel}} + C_{GT,t}^{\mathrm{CTax}}\right)/(1+i)^t, \quad (18)$$

where C_{GT}^{Cap} is the capital cost; C_{GT}^{Sal} is the salvage value, $C_{GT,i}^{\mathrm{O\,\&\,M}}$ is the O&M cost of the tth year; $C_{GT,i}^{\mathrm{Fuel}}$ and $C_{GT,i}^{\mathrm{CTax}}$ are the fuel cost and carbon tax based on fuel consumption, respectively; and i is the discount rate. With the given nominal discount rate i' (the rate at which money is borrowed) and the expected inflation rate f, the real discount rate i can be obtained as follows:

$$i = (i' - f)/(1+f). \quad (19)$$

TABLE I
RELIABILITY COST COMPARISON

	Synchronized grid-connection	Non-synchronized grid-connection
C^{Cap}	$C^1 \times \sum_m P_m^{GT,Max}$	$C^4 \times \sum_m P_m^{GT,Max}$
$C^{Replace}$	Fuse: C^2 per replacement	/
$C^{Unserved}$ (per power outage)	$P^{dem,avg} \times (pT_1 + (1-p)T_2) \times C^{Interrupt}$	/
$C^{Reliability}$ (total)	$C^1 \sum_m P_m^{GT,Max} + \sum_{t=1}^{N} \frac{f_2\left(c^{Replace} + c^{Unserved}\right)}{(1+i)^t}$	$C^4 \sum_m P_m^{GT,Max}$

The modeling of operation constraints, energy consumption, and emissions is similar to what is presented in the operation problem since four representative season days are considered. The operation constraints for the GT mainly include the capacity and heat recovery constraints as in (1) and (4), and energy consumption and emissions as in (2) and (3). In addition, the lifetime constraint is needed. Other devices can be modeled in a similar way. The utility grid can also be treated as a device to the microgrid. Its NPC includes: 1) the capital cost as the interconnection cost for the microgrid to connect to the grid (e.g., device and installation costs); 2) the fuel cost as buying electricity from the grid; and 3) the revenue by selling electricity to the grid. PV uncertainties are not considered in the design problem. This is because the uncertainties will be averaged out as the design time horizon is much longer than the operation one.

2) Modeling of System Balance: In the design problem, the given electricity and thermal demand have to be satisfied for each time slot of the entire microgrid lifetime as in the operation problem.

3) Reliability Cost: The reliability cost includes the capital and replacement costs of fault protection devices such as circuit breakers and fuses to protect the microgrid from the faults coming from the utility grid, and the cost of unserved load during power outages. Here, two types of protection devices are considered. The first type is for synchronized connection with the utility grid such as the current limiting protector [37] and the other is for nonsynchronized connection such as GridLink [38]. For the first type: if the generators of the microgrid fail, the utility grid provides power immediately, and if the utility grid fails, the protection device trips and the power outage occurs. The cost of unserved load can be calculated as the product of the quantity of unserved load $P^{\mathrm{dem,avg}}$ (average load), the interruption duration $T^{\mathrm{Interrupt}}$, and the estimated interruption cost $C^{\mathrm{Interrupt}}$ (\$/kW) [39], that is

$$C^{\mathrm{Unserved}} = P^{\mathrm{dem,avg}} T^{\mathrm{Interrupt}} C^{\mathrm{Interrupt}}. \quad (20)$$

For the second protection device: the power outage only occurs when the generators of the microgrid and the utility grid both fail, whose probability is negligible.

For simplicity, it is assumed that the lifetimes of protection devices are the same as those of microgrids. For illustration

purposes, let the generators of the microgrid fail f_1 times per year and the utility grid fail f_2 times per year. Power outages can be categorized into different types according to different causes. For simplicity, they are categorized into major power outages and general power outages, while the former ones have longer restoration time. It is assumed that $p(\%)$ of the utility grid power outages are major ones with an average restoration time T_1 and the remaining ones are with an average restoration time of T_2. Let C^1 (\$/kW) denote the capital cost of the synchronized protection device and C^2 (\$) and C^3 (\$/kW) the replacement costs of fuses and the device. For the nonsynchronized one, let C^4 (\$/kW) denote its capital cost. For simplicity, the cost of other related devices such as transformers, switchgear, circuit breakers, and protection relay are not considered. This is justified by that the cost of these devices associated with the synchronized grid-connected microgrid is much higher than that associated with the nonsynchronized grid-connected one [40]. With the above data, the reliability costs with the two types of protection devices are compared in Table I.

4) Objective Function: The objective of the design problem is to minimize the lifetime cost of the microgrid, the sum of NPCs of devices (indexed by d) and the net present reliability cost, that is

$$C^{\text{Lifetime}} = \sum_{d}^{C_d^{\text{NPC}}} + C^{\text{Reliability}}. \tag{21}$$

C. Solution Methodology

The problem formulated above is linear and involves both discrete and continuous variables. Since its complexity increases exponentially as the number of device sizes increases, only a limited number of possible combinations of device sizes can be considered. Our idea is to select a certain number of choices for each device based on load profiles. By applying heuristic operation strategies for distributed devices and grid power, the total NPCs of devices under different configurations are evaluated. Then, the net present reliability cost is estimated on the top of it. In this way, the total lifetime costs of different configurations are obtained. In addition, the impacts of uncertain factors such as fuel price and load growth are analyzed through sensitivity analysis.

V. Numerical Results

The method presented above for microgrid operation optimization has been implemented using IBM ILOG CPLEX Optimization Studio V 12.6 [36]. The design method has been implemented using HOMER Pro [41]. Testing has been performed on a PC with a 2.90-GHz Intel Core i7 CPU and a 16-GB RAM. Two examples are presented. The first small classroom example is to illustrate the Markov-based modeling of PV generation in the operation problem and to show different components of the lifetime cost in design. The second semirealistic one based on the Kings Plaza microgrid in Brooklyn, NY, is to show that the operation method is efficient in saving cost and scalable. It is also to compare the lifetime costs of different design configurations and show the impacts of uncertain factors in the design.

Example 1:

In this classroom example, a small microgrid is considered. Devices include the PV, the CCHP (a GT, a steam generator, a steam-driven absorption chiller, and a heat exchanger), an electric chiller, and a boiler. Electricity and natural gas can be used with no limits. A ten-state transition matrix for PV generation is obtained from [30]. The time-varying grid price is taken from [42], where the selling-back price to the grid is set as 90% of the grid price. The natural gas price is obtained from [43]. The carbon intensity of natural gas is based on [44] and the carbon tax is taken from [35]. The results for the operation and design problems are presented in Sections V-A and V-B, respectively.

A. Results for the Operation Problem

The operation problem is for 9 A.M. of a representative summer day in July, where the capacity for the GT is 1600 kW, and 200 kW for the PV. The optimization problem is solved in about 1.5 s. For comparison purposes, an isolated DES with the same energy devices and not connected to the utility grid is considered. In addition, a conventional energy system (Con in Tables) with an electric chiller for space cooling, an electric heater for space heating, and an electric boiler for domestic hot water is also considered. All types of demand are therefore satisfied by the grid power directly or indirectly.

For the microgrid, the total cost is \$-73.35, while the energy cost is \$-89.84 and the carbon tax is \$16.49. The energy cost is negative, which means that the microgrid makes profits by selling electricity back to the grid. For the isolated DES, the total cost is \$98.69, while the energy cost is \$86.16 and the carbon tax is \$12.53. This total cost is much higher than that of the microgrid since the DES cannot buy electricity from the grid or sell electricity to the grid. For the conventional system, the total cost is \$528.68 (no carbon tax), which is much higher than those of the microgrid and DES. This is because during the daytime of summer, the price of grid power is much higher than that of electricity from the CCHP. For these three energy systems, the PV generation levels, GT generation levels, and the grid input under different PV states are shown in Table II. In Table II, grid input equals the amount of electricity from the grid minus the amount of electricity to the grid. The expected device generation levels and grid input of the microgrid and isolated DES are shown in Fig. 2.

Based on Table II, for the microgrid, the GT is always working at the maximum capacity with respect to all PV states. The grid input is negative under all PV states, implying that the microgrid sells electricity back to the grid. When PV generation increases, the amount of electricity to the grid increases since more load is covered by the PV. For the isolated DES, there is no grid input. As PV generation increases, the amount of electricity generated by the GT decreases. For the Con, the grid input is much higher than those of the other two energy systems since all types of demand are covered by the grid power.

According to Fig. 2, for the microgrid, the GT generates more electricity to cover load and sell electricity back to the grid. Space cooling demand is satisfied by the stream-driven chiller with sufficient stream from exhaust heat. For the

TABLE II

EXAMPLE 1: PV AND GT GENERATION LEVELS AND GRID INPUTS UNDER DIFFERENT PV STATES

State	PV gen (kWh)	Microgrid		Isolated DES		Con
		GT gen (kWh)	Grid input (kWh)	GT gen (kWh)	Grid input (kWh)	Grid input (kWh)
1	0	1600	-600	1226.43	0	2173.5
2	14.14	1600	-614.14	1218.50	0	
3	28.28	1600	-628.28	1210.57	0	
4	42.43	1600	-642.43	1202.64	0	
5	56.57	1600	-656.57	1194.70	0	
6	70.71	1600	-670.71	1186.77	0	
7	84.85	1600	-684.85	1178.84	0	
8	98.99	1600	-698.99	1170.91	0	
9	113.14	1600	-713.14	1162.97	0	
10	127.28	1600	-727.28	1155.04	0	

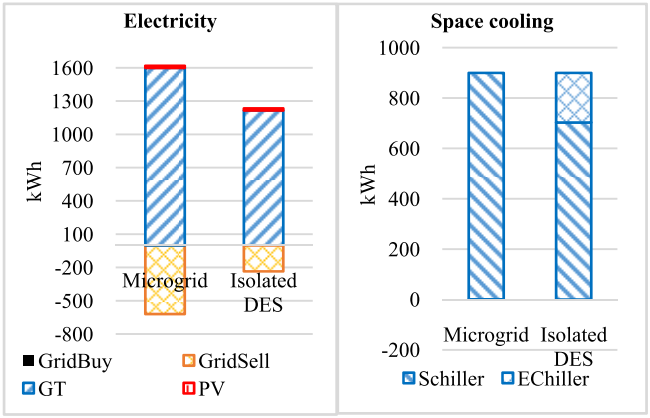

Fig. 2. Example 1: expected device generation levels and grid input.

isolated DES, the GT generates less electricity, just to cover the load and electricity required by the electric chiller. Since the steam is not enough, the electric chiller is used to satisfy the space cooling demand. For domestic hot water, since it can only be met by steam, operation strategies of the heat exchanger are the same for the two energy systems.

B. Results for the Design Problem

HOMER Pro, there are no cooling-related devices, such as absorption or electric chillers. While the cooling provided by the absorption chiller can be converted into the thermal load required by chiller, and the cooling provided by the electric chiller can be converted into the electrical load required by the chiller. The capital and O&M costs of absorption and electric chillers are ignored. In this example, the electricity and thermal loads are scaled from the monthly load profiles provide by HOMER Pro. To make the load data more realistic, it is assumed that the load has an 8% day-to-day variation in each month and an 18% time step-to-step variation in each day. Based on the load profiles, the capacity range for the GT is selected from 1600 to 2000 kW with a 50-kW increase. For PV panels, the capacity range is selected from 100 to 200 kW with a 20-kW increase. The cost-related data of GTs and the PV is obtained from [45], [46], while the energy efficiencies are chosen among typical values. The time-varying grid price and the natural gas price are the same as in the operation problem. The length of the microgrid lifetime is assumed as 20 years. The nominal discount rate i' and the expected inflation rate f are

TABLE III

EXAMPLE 1: TOTAL LIFETIME COSTS OF DIFFERENT MICROGRID CONFIGURATIONS

Type	GT + PV (kW)	Grid-connection	$C^{Cap}+C^{Replace}$ (M$)	$C^{O\&M}$ (M$)	C^{Fuel} (M$)	C^{Grid} (M$)	C^{CTax} (M$)	$C^{Reliability}$ (M$)	C^{NPC} (M$)
Micro-grid	1600+100	Syn	9.12	2.07	10.31	-11.28	1.5	2.71	14.28
		Non	9.12	2.07	10.31	-11.28	1.5	1.2	12.77
	1600+200	Syn	9.33	2.09	10.31	-11.56	1.5	2.71	14.21
		Non	9.33	2.09	10.31	-11.56	1.5	1.2	12.71
	1800+100	Syn	9.98	2.32	11.56	-13.83	1.68	2.85	14.41
		Non	9.98	2.32	11.56	-13.83	1.68	1.35	12.91
	1800+200	Syn	10.19	2.35	11.56	-14.11	1.68	2.85	14.35
		Non	10.19	2.35	11.56	-14.11	1.68	1.35	12.85
	2000+100	Syn	10.83	2.58	12.81	-16.37	1.86	2.99	14.54
		Non	10.83	2.58	12.81	-16.37	1.86	1.5	13.05
	2000+200	Syn	11.05	2.6	12.81	-16.65	1.86	2.99	14.48
		Non	11.05	2.6	12.81	-16.65	1.86	1.5	12.99
Isolated DES	1600+200	/	7.33	2.07	5.13	0	0.77	2.19	17.33
Con	/	/	0	0	0	20.26	0	1.3	21.56

TABLE IV

EXAMPLE 1: RELIABILITY COSTS FOR DIFFERENT ENERGY SYSTEMS

	Synchronized connection	Non-Synchronized connection	Isolated DES	Conventional system
C^{Cap}	79.5 [54] × 1600 = $0.127M	750 [56] × 1600 = $1.2M	/	/
$C^{Replace}$	Fuse: $0.045M per replacement [54] Device: 29 [54] × 1600=$0.0464M	/	/	/
$C^{Unserved}$ (per power outage)	518 × (38% × 8+ 62% × 2) ×12.1 ([55])=$0.027M	/	518 × 4 × 12.1 = $0.025M	1164 × (38% × 8+ 62% × 2) × 12.1 = $0.06M
$C^{Reliability}$	$2.71M	$1.2M	$2.19M	$1.3M

4.98% and 1.68% (the average values of the monthly interest and inflation rates in the past six years [47], [48]), respectively. Then, the real discount rate i is 3.25% based on (19).

To calculate the reliability costs, it is assumed that the microgrid generator fails six times per year [49] and the utility grid fails 1.5 times per year [50]. Based on the outage records of Northeast Utilities, 38% of the power outage was caused by windstorms with an average restoration time of 8 h, and the resting has an average restoration time of 2 h [51]. For comparison purposes, the isolated DES and the conventional system mentioned in the operation problem are also considered here. For the isolated DES, the interruption duration is assumed as 4 h [52].

1) Total Lifetime Costs: The total NPCs of devices under different configurations of the microgrid under consideration are evaluated in HOMER Pro, while the net present reliability costs are estimated on the top of it. Then, the lifetime cost of each selected configuration is obtained as shown in Table III, as well as those of the isolated DES and the conventional system with specific configurations (the capital and O&M costs of electrical devices in the conventional system are ignored). For illustration purposes, the results for the configurations with the GT of 1600, 1800, and 2000 kW and the PVs of 100 and 200 kW are presented.

Each configuration of the microgrid under consideration has a lower lifetime cost than those of the isolated DES and the conventional system, no matter synchronized or nonsynchronized grid connection, although there is a high grid interconnection cost ($2M, scaled from [53]). This is mainly because the microgrid can make profits by selling electricity to the grid when the grid price is high. For the same configuration of the microgrid, the lifetime cost of the nonsynchronized grid connection is lower than that of the synchronized grid connection, which will be explained later. The best configuration with the lowest lifetime cost is the one with a GT of 1600 kW and PV panels of 200 kW. The conventional system has the highest lifetime cost.

2) Reliability Costs: To show how the total reliability costs are calculated in Table III, the details are discussed here. For the microgrid, each part in the total reliability cost is explained in Table I. For the isolated DES, no protection devices are needed to prevent the faults from the utility grid. When the generator goes down and there is no power supply, the cost of unserved load occurs, which is calculated by (20). Since there are no distributed generators in the conventional system, no protection devices are needed either. When the grid goes down, there will be costs of unserved load. The reliability costs of the microgrid with a GT of 1600 kW and PV panels of 200 kW under two types of grid connection, and those of the isolated DES (the same device configuration as the microgrid) and the conventional system with no protection devices are compared in Table IV.

Under the synchronized grid connection, the total reliability cost is $2.71M, while the total reliability cost is $1.2M under the nonsynchronized grid connection. Although the capital cost of the protection device for the nonsynchronized connection is very high as compared with that for the synchronized connection, the cost of unserved load is 0. For the isolated DES, since there is no protection device, its total reliability cost is much lower than that of the microgrid. The conventional system has a higher reliability cost than the isolated DES since the average electrical load of the conventional system is higher as all types of demand are satisfied by grid power.

Example 2:

This example is semirealistic based on the microgrid of Kings Plaza in Brooklyn, NY. It is to show that the total energy and emission cost can be reduced by the optimized operation of the microgrid and to compare the lifetime costs of different design configurations and show the impacts of uncertain factors in the design. In this example, all devices mentioned in Section III are considered. The cost related data is the same as in the first example. The hourly electricity, space heating and cooling, and demand domestic hot water demand of four representative days are built based on [57]–[60]. For each representative season day, the hourly energy demand is calculated as the average of the energy demand in the corresponding hour of all days in this season. The stop mixed-integer programming gap is 0.5% for the operation problem. The results for the operation and design problems are presented in Sections V-C and V-D, respectively.

C. Results for the Operation Problem

In the operation problem, the total capacity for GTs is 6400, 500 kW for the PV, and 500 kW for the battery. For a winter day with 1 h as a time interval, the daily cost of the microgrid under consideration is $3,583/day, while the energy cost is $2,436/day, whereas the carbon tax is $1,147/day. For comparison purposes, an isolated DES with the same device configuration is considered, as well as the conventional system mentioned in Example 1. For the isolated DES, the daily cost is $6,264/day, while the energy cost is $5,469/day and the carbon tax is $795/day. For the conventional system, the daily cost is $13,663/day (no carbon tax). Among the three energy systems, the microgrid has the lowest daily cost by using grid power or distributed energy devices whichever is cheaper.

To analyze the optimized operation strategies, a particular scenario of PV generation is presented in the following. To demonstrate that the total energy and emission cost can be reduced by the optimized operation of the microgrid, the total costs of each representative season day under the optimized and heuristic operations are compared. The Monte Carlo simulation is also performed on these four days.

1) Optimized Operation Strategies for a Particular Scenario: The particular scenario in the typical winter day is selected, where the PV generation at each time is at state 5. By solving the operation optimization problem for this scenario, the hourly electrical load, electricity provided by CCHP, grid input, and grid power price are shown in Fig. 3.

When the grid price is low, e.g., from 0:00 to 5:00, the grid input is positive and the microgrid buys electricity to cover the entire electrical load. During 6:00 to 7:00, the CCHP begins to generate electricity and the grid input decreases. When the grid price is high since 8:00, the CCHP generates electricity at its maximum capacity to cover the load and to sell to the grid, so the grid input is negative. In addition, PV panels also cover partial electrical load during the daytime.

2) Optimized and Heuristic Operation Strategies: To evaluate the optimized operation strategies, the heuristic operation strategies are also considered. For the CCHP, the selected heuristic strategies are as follows: four engines during the daytime in summer and three in other seasons and two engines from 23:00 to 7:00. For the battery, it is assumed that it charges during the daytime and discharges at night under the heuristic operation strategy. For a typical day in each season, the daily costs with the optimized and heuristic operation strategies are compared in Table V. The CPU time is also presented.

For each season, the daily cost is reduced by more than 40% under the optimized operation compared with that obtained under the heuristic operation. The relative difference between the daily costs obtained by the optimized and heuristic operations in summer is the largest among the four seasons. This is because the microgrid makes more profits by the optimized operation in summer when the grid price is very high. For this problem, the CPU time is about 9 s, while it is 1.5 s for the 1-h problem in Example 1. The computational time is nearly linear to the problem size. Therefore, the method is efficient in saving cost and scalable for large microgrids.

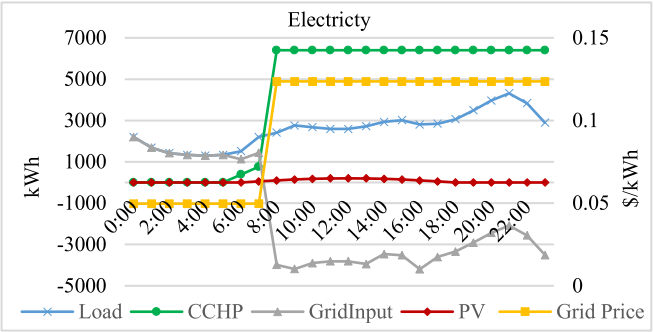

Fig. 3. Example 2: hourly grid price, electrical load, electricity provided by the CCHP, and grid input.

TABLE V
EXAMPLE 2: OPTIMIZED AND HEURISTIC OPERATIONS OF THE MICROGRID

Season	Operation strategy	Energy cost ($)	Carbon tax ($)	Total cost ($)	CPU time (s)
Spring	Optimized	2,117	1,097	3,214	8.2
	Heuristic	3,631	1,008	4,639	/
Summer	Optimized	-2,856	1,117	-1,739	9.3
	Heuristic	-2,011	1,241	-770	/
Fall	Optimized	2,532	1,117	3,649	9.5
	Heuristic	4,441	993	5,434	/
Winter	Optimized	2,436	1,147	3,583	8.6
	Heuristic	4,049	1,073	5,122	/

TABLE VI
EXAMPLE 2: SIMULATION RESULTS FOR THE MICROGRID OPERATION

Season	Simulation cost ($)	Optimization cost ($)	APE (%)	STD ($)
Spring	3,213	3,214	0.03	1.21
Summer	-1,752	-1,739	0.76	8.75
Fall	3,646	3,649	0.09	1.74
Winter	3,580	3,583	0.10	1.45

3) Monte Carlo Simulation: To evaluate the optimization results, 1000 Monte Carlo simulation runs are performed with ten-state transition matrices for the four typical season days. Modeling accuracy is measured by the absolute percentage error (APE), the ratio of the absolute difference between the optimization and simulation costs to the simulation cost. The standard deviation (STD) of scenario costs reflects its variation. The results of the four typical season days are summarized in Table VI.

It can be seen that the APEs are all within 1% for all seasons, demonstrating the modeling accuracy. The APE and STD in summer are the largest among the four seasons, since the variation of PV generation is the largest in summer in this example.

D. Results for the Design Problem

For the design problem, the cost related data including the reliability costs is the same as in Example 1, and the cost of the battery is taken from [61]. The hourly load is obtained based on the four typical days mentioned in the operation problem above. Similar to Example 1, an 8% day-to-day variation in each season and an 18% time step-to-step variation in each day are considered. Based on the load profiles, the capacity range for each GT is selected from 1600 to 3200 kW with a 400-kW increase. As for PV panels, its total capacity range is selected from 200 to 500 kW with a 50-kW increase. The battery is from 200 to 500 kW with a 50-kW increase. When the grid price is high, grid power is not allowed to charge the battery, and when the price is low, the battery cannot discharge for selling electricity to the grid. The lifetime of the microgrid is assumed as 20 years. In this section, the lifetime costs of different configurations are compared. The impacts of uncertain factors, load and fuel prices, are also discussed.

TABLE VII
EXAMPLE 2: LIFETIME COSTS OF DIFFERENT MICROGRID CONFIGURATIONS

Type	GT + PV +Battery (kW)	Grid-connection	$C^{Cap}+C^{Replace}$ (M$)	$C^{O\&M}$ (M$)	C^{Fuel} (M$)	C^{Grid} (M$)	C^{CTax} (M$)	$C^{Reliability}$ (M$)	C^{NPC} (M$)
Microgrid	6400+20	Syn	30.60	12.44	27.2	-16.52	3.96	8.34	56.8
	0 + 500	Non	31.33	11.67	28.25	-16.52	3.96	4.8	53.82
	6400+50	Syn	31.07	12.48	27.09	-17.19	3.94	8.34	56.46
	0 + 500	Non	31.07	12.48	27.09	-17.19	3.94	4.8	52.92
	9600+20	Syn	38.98	15.70	34.00	-36.89	4.95	10.62	53.85
	0 + 500	Non	38.98	15.70	34.00	-36.89	4.95	7.2	50.43
	9600+50	Syn	39.45	15.77	33.96	-37.67	4.94	10.62	53.51
	0 + 500	Non	39.45	15.77	33.96	-37.67	4.94	7.2	50.1
	12800+2	Syn	44.86	19.49	42.01	-59.11	6.11	12.89	51.23
	00 + 500	Non	44.86	19.49	42.01	-59.11	6.11	9.6	47.94
	12800+5	Syn	45.34	19.57	42.00	-59.94	6.11	12.89	50.9
	00 + 500	Non	45.34	19.57	42.00	-59.94	6.11	9.6	47.61
	12800+5	Syn	45.24	19.46	42.01	-60.40	6.11	12.89	50.27
	00 + 200	Non	45.24	19.46	42.01	-60.40	6.11	9.6	46.98
Isolated DES	12800+500	/	33.34	5.40	23.62	0	3.44	2.85	61.99
Con	/	/	0	0	0	70.3	0	4.95	75.22

1) Total Costs: By solving the design problem, the total lifetime costs of selected configurations of the microgrid under consideration are presented in Table VII. As in Example 1, it is assumed that each microgrid generator fails six times per year [49] and the four generators are parallel. According to fault tree analysis, the overall CHP fails 1.64 times per year [62]. The utility grid fails 1.5 times per year [50]. The total lifetime costs of the isolated DES and the conventional system with specific configurations (the capital and O&M costs of electrical devices in the conventional system are ignored) are also considered. For illustration purposes, the configurations with the total GT capacities of 6400, 9600, and 12800 kW, the PVs of 200 and 500 kW, and the battery of 500 kW are selected and presented. In addition, the configurations with a total GT capacity of 12800 kW, PV panels of 500 kW, and the battery of 200 kW are also presented.

The comparison among the three systems is similar to that of Example 1. The microgrid has the lowest lifetime cost although the capital cost is high, and the conventional system has the highest one. While for the same microgrid configuration, the lifetime cost with the nonsynchronized grid connection is lower than that under the synchronized grid connection. Different from Example 1, the higher the total capacity of GTs, the lower the total lifetime cost of the microgrid. This is because the additional profits made by selling electricity to the grid exceed the additional costs

TABLE VIII
EXAMPLE 2: SENSITIVITY ANALYSIS

Natural gas price	Average Load	Grid -Con	Total lifetime cost (M$)	Compared with the nominal (%)
0.27$/m^3	2,479kW	Syn	50.9	/(Nominal)
		Non	47.61	/(Nominal)
	2,727kW (10% increase)	Syn	54.91	7.88
		Non	51.62	8.42
0.297$/m^3 (10% increase)	2,479kW	Syn	55.37	8.78
		Non	51.79	8.78
	2,727kW (10% increase)	Syn	59.4	16.7
		Non	55.83	17.27

(e.g., O&M and reliability costs), opposite to Example 1. In addition, based on the last two microgrid configurations with different battery sizes, the higher the capacity of the battery, the higher the total lifetime cost of the microgrid. In daily operation, the battery can provide electricity when the Sun is covered by clouds to dampen the intermittency of PVs. Here the PV generation is deterministic, where its uncertainties are not involved. Also since heuristic operation strategies are considered in the design problem, the economic benefits of batteries are not fully explored. In summary, the best design with the lowest lifetime cost is the configuration with a total GT capacity of 12800 kW, PV panels of 500 kW, and the battery of 200 kW.

In the operation problem, for the microgrid with a total GT capacity of 6400 kW, PV panels of 500 kW, and battery of 500 kW, the daily costs of each seasons are obtained as shown in Table V. With the interest rate mentioned in Example 1 and the length of each season, the sum of the total energy cost and carbon tax over the lifetime is approximated as $10.8M and $18.0M under the optimized and heuristic operations. While in the design problem, this number is $13.8M ($C^{\text{Fuel}} + C^{\text{Grid}} + C^{\text{CTax}}$) based on Table VII. This implies that the lifetime energy and emission cost is significantly reduced by the optimized operation.

2) Effects of Uncertain Factors: To evaluate the effects of fuel price and load growth, sensitivity analysis is performed on two values for the natural gas price and two for the average electrical load. With the four combinations, the lifetime costs for the microgrid with a total GT capacity of 12800 kW, PV panels of 500 kW, and battery of 200 kW are compared in Table VIII.

Under both synchronized and nonsynchronized grid connections, fuel price growth has a little bit more effects on the total lifetime cost than load growth. This is because the profits made by the microgrid are closely related to the fuel price. The natural gas price almost has the same effects on the lifetime costs under two types of grid connections, while load growth has more under the nonsynchronized grid connection.

VI. IMPLICATIONS FOR REGULATORS AND DISTRIBUTION UTILITIES

The implications of the above models, methods, and results on the operation and design of microgrids with renewables for regulators and distribution utilities are discussed below.

Historically, electric power distribution companies (DISCOs) have been working as investor-owned regulated monopolies in the U.K. and many states in the U.S. DISCOs own and operate distribution infrastructures to provide unidirectional delivery of power from upstream merchant generators to downstream consumers. This unidirectional engineering and transactional arrangement is often referred as a cost-of-service business model. Cost-of-service regulators require DISCOs to approximate the optimal investment and operation of the distribution network using discounted cash flow tools or net present value analysis as standard approaches for investment decision making [63]. However, once the investment decision is made, the net present value approach assumes that there is no scope for managers to react to new information, although in practice many investments confer future options and management flexibility. In addition, the net present value approach ignores flexibility with regard to timing of an investment decision. Its static nature means that it systematically undervalues investment opportunities that provide future options. Under certain circumstances, e.g., significant uncertainty and flexibility, the net present value approach can lead to poor policy and investment decisions.

More recently, national regulators in the U.K. and state regulators in New York and California have begun implementing performance-based regulatory reform to convert DISCOs into a bi-directional two-sided platform business model. This platform enables downstream customers who install more reliable, less expensive, and more environmentally sustainable distributed generation to interconnect to and transact with the utility grid, the same as what presented in the previous sections. The downstream customers can sell spinning reserves, demand response, and power quality services to the distribution network and buy standby power from the network. DISCOs will earn income from the performance of the engineering and transactional platforms that they own and manage [64], [65].

Under the two-sided platform business model, most DISCOs in the U.K. use approaches similar to real option analysis to account for the flexibility of distributed energy resources [65]. Real option analysis (based on Monte Carlo simulations) seeks to value flexibility embedded within the investment option and flexibility of delaying the investment through time [63]. So far, New York and California regulators have persisted in the use of less accurate discounted cash flow techniques from cost-of-service regulation to approximate the resource optimization in two-sided platform business models mandated by the performance-based regulatory reform [67], [68].

Beyond the methods mentioned above, some regulators and DISCOs are still looking for efficient optimization tools. The optimization models, methods, and results demonstrated in this paper show that appropriate modeling and efficient optimization methods can deliver accurate optimization results with off-the-shelf computational tools (e.g., CPLEX and HOMER Pro) and does not increase the complexity of the tools used by regulators and DISCO planners.

VII. CONCLUSION

This paper investigates operation and design optimization of microgrids. From the energy and emission point of view, a mixed-integer model is established for operation. PV uncer-

tainties are modeled by a Markovian process. For effective coordination, other devices are modeled as Markov processes with states depending on PV states. The entire problem is Markovian and solved using branch-and-cut. For design, a linear model is established to evaluate the microgrid lifetime cost, where the reliability cost is obtained based on the microgrid configuration and the cost of unserved load during power outages. With a limited number of possible combinations of device sizes, exhaustive search is used to find the optimized design. The numerical results show that the operation method is efficient in saving cost and scalable and microgrids have lower lifetime costs than conventional energy systems. The optimization models, methods, and results demonstrated in this paper show that appropriate modeling and efficient optimization methods can deliver accurate optimization results with off-the-shelf computational tools without increasing the complexity of the tools used by regulators and DISCO planners.

REFERENCES

[1] N. Hatziargyriou, H. Asano, R. Iravani, and C. Marnay, "Microgrids," *IEEE Power Energy Mag.*, vol. 5, no. 4, pp. 78–94, Jul./Aug. 2007.

[2] F. Katiraei and M. R. Iravani, "Power management strategies for a microgrid with multiple distributed generation units," *IEEE Trans. Power Syst.*, vol. 21, no. 4, pp. 1821–1831, Nov. 2006.

[3] X. Guan, Z. Xu, and Q.-S. Jia, "Energy-efficient buildings facilitated by microgrid," *IEEE Trans. Smart Grid*, vol. 1, no. 3, pp. 243–252, Dec. 2010.

[4] S. Mohammadi, S. Soleymani, and B. Mozafari, "Scenario-based stochastic operation management of microgrid including wind, photovoltaic, micro-turbine, fuel cell and energy storage devices," *Int. J. Elect. Power Energy Syst.*, vol. 54, pp. 525–535, Jan. 2014.

[5] Siemens AG. *Virtual Power Plants by Siemens*. accessed on Oct. 21, 2016, [Online]. Available: https://w3.usa.siemens.com/smartgrid/us/en/distributech/Documents/DEMS_VPPs.pdf.

[6] Y. H. Chen, S. Y. Lu, Y. R. Chang, T. T. Lee, and M. C. Hu, "Economic analysis and optimal energy management models for microgrid systems: A case study in Taiwan," *Appl. Energy*, vol. 103, pp. 145–154, Mar. 2013.

[7] H. Morais, P. Kádár, P. Faria, Z. A. Vale, and H. M. Khodr, "Optimal scheduling of a renewable micro-grid in an isolated load area using mixed-integer linear programming," *Renew. Energy*, vol. 35, no. 1, pp. 151–156, 2010.

[8] D. E. Olivares, J. D. Lara, C. A. Cañizares, and M. Kazerani, "Stochastic-predictive energy management system for isolated microgrids," *IEEE Trans. Smart Grid*, vol. 6, no. 6, pp. 2681–2693, Nov. 2015.

[9] M. Ross, R. Hidalgo, C. Abbey, and G. Joós, "Energy storage system scheduling for an isolated microgrid," *IET Renew. Power Generat.*, vol. 5, no. 2, pp. 117–123, Mar. 2011.

[10] R. Palma-Behnke *et al.*, "A microgrid energy management system based on the rolling horizon strategy," *IEEE Trans. Smart Grid*, vol. 4, no. 2, pp. 996–1006, Jun. 2013.

[11] A. Parisio, E. Rikos, and L. Glielmo, "A model predictive control approach to microgrid operation optimization," *IEEE Trans. Control Syst. Technol.*, vol. 22, no. 5, pp. 1813–1827, Sep. 2014.

[12] T. Niknam, R. Azizipanah-Abarghooee, and M. R. Narimani, "An efficient scenario-based stochastic programming framework for multi-objective optimal micro-grid operation," *Appl. Energy*, vol. 99, pp. 455–470, Nov. 2012.

[13] M. Hemmati, N. Amjady, and M. Ehsan, "System modeling and optimization for islanded micro-grid using multi-cross learning-based chaotic differential evolution algorithm," *Int. J. Elect. Power Energy Syst.*, vol. 56, pp. 349–360, Mar. 2014.

[14] B. Zhao, X. Zhang, J. Chen, C. Wang, and L. Guo, "Operation optimization of standalone microgrids considering lifetime characteristics of battery energy storage system," *IEEE Trans. Sustain. Energy*, vol. 4, no. 4, pp. 934–943, Oct. 2013.

[15] A. D. Hawkes and M. A. Leach, "Modelling high level system design and unit commitment for a microgrid," *Appl. Energy*, vol. 86, nos. 8–9, pp. 1253–1265, Aug. 2009.

[16] H. Ren and W. Gao, "A MILP model for integrated plan and evaluation of distributed energy systems," *Appl. Energy*, vol. 87, no. 3, pp. 1001–1014, 2010.

[17] K. A. Pruitt, R. J. Braun, and A. M. Newman, "Evaluating shortfalls in mixed-integer programming approaches for the optimal design and dispatch of distributed generation systems," *Appl. Energy*, vol. 102, pp. 386–398, Feb. 2013.

[18] Y. A. Katsigiannis, P. S. Georgilakis, and E. S. Karapidakis, "Multiobjective genetic algorithm solution to the optimum economic and environmental performance problem of small autonomous hybrid power systems with renewables," *IET Renew. Power Generat.*, vol. 4, no. 5, pp. 404–419, Sep. 2010.

[19] O. Hafez and K. Bhattacharya, "Optimal planning and design of a renewable energy based supply system for microgrids," *Renew. Energy*, vol. 45, pp. 7–15, Sep. 2012.

[20] M. J. Khan and M. T. Iqbal, "Pre-feasibility study of stand-alone hybrid energy systems for applications in Newfoundland," *Renew. Energy*, vol. 30, no. 6, pp. 835–854, May 2005.

[21] J. Cotrell and W. Pratt, "Modeling the feasibility of using fuel cells and hydrogen internal combustion engines in remote renewable energy systems," Nat. Renew. Energy Lab., Golden, CO, USA, Tech. Rep. NREL/TP-500-34648, Sep. 2003.

[22] T. Givler and P. Lilienthal, "Using HOMER software, NRELs micropower optimization model, to explore the role of gen-sets in small solar power systems," Nat. Renew. Energy Lab., Golden, CO, USA, Tech. Rep. NREL/TP-710-36774, May 2005.

[23] R. Dufo-López *et al.*, "Multi-objective optimization minimizing cost and life cycle emissions of stand-alone PV–wind–diesel systems with batteries storage," *Appl. Energy*, vol. 88, no. 11, pp. 4021–4022, 2011.

[24] R. Dufo-López and J. L. Bernal-Agustin, "Multi-objective design of PV–wind–diesel–hydrogen–battery systems," *Renew. Energy*, vol. 33, no. 12, pp. 2259–2272, 2008.

[25] P. B. Luh *et al.*, "Grid integration of intermittent wind generation: A Markovian approach," *IEEE Trans. Smart Grid*, vol. 5, no. 2, pp. 732–741, Mar. 2014.

[26] M. di Somma *et al.*, "Operation optimization of a distributed energy system considering energy costs and exergy efficiency," *Energy Convers. Manage.*, vol. 103, pp. 739–751, Oct. 2015.

[27] M. di Somma *et al.*, "Multi-objective operation optimization of a distributed energy system for a large-scale utility customer," *Appl. Thermal Eng.*, vol. 101, pp. 752–761, May 2016.

[28] B. Yan *et al.*, "Exergy-based operation optimization of a distributed energy system through the energy-supply chain," *Appl. Thermal Eng.*, vol. 101, pp. 741–751, May 2016.

[29] X. Q. Kong, R. Z. Wang, and X. H. Huang, "Energy optimization model for a CCHP system with available gas turbines," *Appl. Thermal Eng.*, vol. 25, nos. 2–3, pp. 377–391, 2005.

[30] P. S. Perez, J. Driesen, and R. Belmans, "Characterization of the solar power impact in the grid," in *Proc. Int. Conf. Clean Elect. Power*, Capri, Italy, May 2007, pp. 366–371.

[31] W. Palz, *Photovoltaic Power Generation*. Amsterdam, The Netherlands: Reidel, 1982, p. 45.

[32] P. Poggi, G. Notton, M. Muselli, and A. Louche, "Stochastic study of hourly total solar radiation in Corsica using a Markov model," *Int. J. Climatol.*, vol. 20, no. 14, pp. 1843–1860, Nov. 2000.

[33] B. O. Ngoko, H. Sugihara, and T. Funaki, "Synthetic generation of high temporal resolution solar radiation data using Markov models," *Solar Energy*, vol. 103, pp. 160–170, May 2014.

[34] C. Weber, P. Meibom, R. Barth, and H. Brand, "WILMAR: A stochastic programming tool to analyze the large-scale integration of wind energy," in *Optimization in the Energy Industry*, vol. 19. Berlin, Germany: Springer, 2009, pp. 437–458.

[35] *Center for Climate and Energy Solutions, Options and Considerations For a Federal Carbon Tax*, accessed on Feb. 22, 2016. [Online]. Available: http://www.c2es.org/publications/options-considerations-federal-carbon-tax

[36] *IBM, IBM ILOG CPLEX Optimization Studio CPLEX User's Manual*, Sunnyvale, CA, USA.

[37] *Current Limiting Protector (CLiP)*, accessed on Nov. 13, 2014. [Online]. Available: http://www.gwelec.com/current-limiting-protector-clip-p-102-l-en.html

[38] *A Better Way to Integrate Distributed Energy Resources and the Grid*, accessed on Jan. 25, 2015. [Online]. Available: http://www.paretoenergy.com/our-tech/

[39] M. A. Ortega-Vazquez and D. S. Kirschen, "Optimizing the spinning reserve requirements using a cost/benefit analysis," *IEEE Trans. Power Syst.*, vol. 22, no. 1, pp. 24–33, Feb. 2007.

[40] Pareto Energy, "GridLink: A new power electronics interconnection technology study final report," New York State Energy Res. Develop. Authority, Albany, NY, USA, Tech. Rep., Nov. 2014.

[41] *HOMER Energy*. [Online]. Available: http://www.homerenergy.com

[42] Consolidated Edison, accessed on Jan. 28, 20116. [Online]. Available: https://apps.coned.com/CEMyAccount/csol/MSCcc.aspx

[43] (Jun. 2014). *New York Price of Natural Gas Sold to Commercial Consumers*. [Online]. Available: http://www.eia.gov/dnav/ng/hist/n3020ny3m.htm

[44] Educogen, *The European Educational Tool on Cogeneration*, 2nd ed. Belgium, U.K.: European Association for the Promotion of Cogeneration, 2001.

[45] *CHP Database: SENTECH Incorporated—C&I CHP Technology Cost and Performance Data Analysis for EIA*, U.S. Energy Inf. Admin., Washington, DC, USA, Jun. 2010.

[46] National Renewable Energy Laboratory. *Distributed Generation Renewable Energy Estimate of Costs*, accessed on Feb. 17, 2016. [Online]. Available: http://www.nrel.gov/analysis/tech_lcoe_re_cost_est.html

[47] *SBA 504 Rate Archive*, accessed on Feb. 29, 2016. [Online]. Available: http://cdcloans.com/lender/504-rate-history/504-rate-archive/

[48] *Historical Inflation Rate*, accessed on Feb. 29, 2016. [Online]. Available: http://inflationdata.com/Inflation/Inflation_Rate/HistoricalInflation.aspx

[49] R. K. Wassan, M. A. A. Majid, and A. A. Mokhtar, "Impact of different repair assumptions on repairable system risk assessment," *Res. J. Appl. Sci. Eng. Technol.*, vol. 4, no. 7, pp. 870–874, 2014.

[50] (2015). *EIA Annual Electric Power Industry Report*. [Online]. Available: https://www.eia.gov/todayinenergy/detail.php?id=27892

[51] G. Li *et al.*, "Risk analysis for distribution systems in the Northeast U.S. under wind storms," *IEEE Trans. Power Syst.*, vol. 29, no. 2, pp. 889–898, Mar. 2014.

[52] *Assessment of the GridLink Technology*, Univ. Connecticut, Storrs, CT, USA, Jul. 2015.

[53] (2014). *State of New York Public Service Commission, Proceeding on Motion of the Commission in Regard to Reforming the Energy Vision*. [Online]. Available: http://documents.dps.ny.gov/public/Common/ViewDoc.aspx?DocRefId=%7BCFC6F0D9-6E64-4196-9AC7-1A199132DF5B%7D

[54] *New York State Energy Research and Development Authority, New York Presbyterian Hospital Combined Heat and Power Project: Commutating 1216 Current Limiter Electric Power Transmission and Distribution (EPTD) Program*, Brooklyn, NY, USA, 2010.

[55] M. J. Sullivan, J. A. Schellenberg, and M. G. Mercurio, "Updated value of service reliability estimates for electric utility customers in the United States," Lawrence Berkeley Nat. Lab. Res. Project Final Rep., Berkeley, CA, USA, Tech. Rep., Jan. 2015. [Online]. Available: http://eetd.lbl.gov/sites/all/files/lbnl-6941e_0.pdf

[56] Pareto Energy. *Microgrids for Data Centers*, accessed on Nov. 3, 2014. [Online]. Available: http://www.paretoenergy.com/whitepaperfiles/PresentationParetoEnergyMicrogridsForDataCenters WebPageVersion.pdf

[57] *EPBD Buildings Platform. Country Reports*, 2008.

[58] L. Mongibello, N. Bianco, M. Caliano, and G. Graditi, "Influence of heat dumping on the operation of residential micro-CHP systems," *Appl. Energy*, vol. 160, pp. 206–220, Dec. 2015.

[59] M. Bianchi, A. de Pascale, and P. R. Spina, "Guidelines for residential micro-CHP systems design," *Appl. Energy*, vol. 97, pp. 673–685, Sep. 2012.

[60] E. S. Barbieri, F. Melino, and M. Morini, "Influence of the thermal energy storage on the profitability of micro-CHP systems for residential building applications," *Appl. Energy*, vol. 97, pp. 714–722, Sep. 2012.

[61] R. Carnegie, D. Gotham, D. Nderitu, and P. V. Preckel, *Utility Scale Energy Storage Systems, Benefits, Applications, and Technologies*. West Lafayette, IN, USA: Purdue Univ., 2013, p. 48.

[62] M. Rausand and A. Høyland, *System Reliability Theory: Models, Statistical Methods, and Applications*, vol. 396. Hoboken, NJ, USA: Wiley, 2004.

[63] J. Grayburn, "Real options and investment decision making consultation," United Kingdom Office Gas Electr. Markets, London, U.K., Tech. Rep., 2012.

[64] Y. D. Lee and S. Y. Park, "Reactive power support capabilities of nonsynchronous interconnection systems in microgrid applications," in *Proc. IEEE Appl. Power Electron. Conf. Expo. (APEC)*, Long Beach, CA, USA, Mar. 2016, pp. 125–131.

[65] New York Public Service Commission, *Request for Three Regulatory Rulings on a Project Financing and Profit Sharing Plan for Demonstrating a Two-Sided Microgrid Platform Business Model in Brooklyn and Queens, Case 15-E-0250 Proceeding on Motion of the Commission in Regard to Petition of Pareto Energy Ltd. to Implement a Microgrid Business Model as a Least-Cost Resource to Meet Reliability Contingencies and Demand Management Objectives at Consolidated Edison*, New York, NY, USA, Dec. 2015.

[66] J. Grayburn, "Real options: An application to gas network interruptible contract auctions," United Kingdom Office Gas Electr. Markets, London, U.K., Tech. Rep., 2012.

[67] California Public Utilities Commission, *Assigner Commissioners Ruling on Guidance for Public Utilities Code Section 769—Distribution Resource Planning, Rulemaking 14-08-013 Order Instituting Rulemaking Regarding Policies, Procedures and Rules for Development of Distribution Resources Plans Pursuant to Public Utilities Code Section 769*, San Francisco, CA, USA, Aug. 2014.

[68] New York State Public Service Commission, *Order Establishing Benefit Cost Analysis Framework, Case 14-M-0101 Proceeding on the Motion of the Commission in Regard to Reforming the Energy Vision*, New York, NY, USA, Jan. 2016.

Bing Yan (S'11–M'17) received the B.S. degree from the Renmin University of China, Beijing, China, in 2010, and the M.S. and Ph.D. degrees from the University of Connecticut, Storrs, CT, USA, in 2012 and 2016, respectively.

Her research interests include operation and design optimization of microgrids, grid integration of renewables (wind and solar), exergy-based operation optimization of distributed energy systems, and scheduling of manufacturing systems.

Peter B. Luh (S'77–M'80–SM'91–F'95) received the B.S. degree from National Taiwan University, Taipei, Taiwan, in 1973, the M.S. degree from the Massachusetts Institute of Technology, Cambridge, MA, USA, in 1977, and the Ph.D. degree from Harvard University, Cambridge, in 1980.

Since 1980, he has been with the University of Connecticut, Storrs, CT, USA, where he is currently the SNET Professor of Communications and Information Technologies. His interests include smart power systems-smart grid, design of auction methods for electricity markets, effective renewable (wind and solar) integration to the grid, electricity load and price forecasting with demand response, and micro grid.

Dr. Luh was the Vice President of Publication Activities for the IEEE Robotics and Automation Society.

Guy Warner received the B.A. degree in government from St. Lawrence University, Canton, NY, USA, in 1979, and the graduate courses in mixed-integer financial and regulatory optimization models from George Washington University, Washington, DC, USA.

Since that time, he has applied the techniques in a wide variety of commercial applications, including computable general equilibrium models for debt restructuring by central banks in several Latin American countries in the 1980s, gas supply optimization models to respond to deregulation of gas distribution company deregulation in the 1990s, and distributed energy resource optimization models to adapt to two-sided electric utility business models in the last 15 years.

Peng Zhang (M'07–SM'10) received the Ph.D. degree in electrical engineering from the University of British Columbia, Vancouver, BC, Canada, in 2009.

He is currently an Assistant Professor of Electrical Engineering with the University of Connecticut, Storrs, CT, USA. He was a System Planning Engineer at BC Hydro and Power Authority, Vancouver. His research interests include active distribution network, microgrids, smart city, renewable energy systems, power system resilience and reliability, and software defined networking.

Dr. Zhang is a Registered Professional Engineer in BC, Canada, and a member of CIGRÉ.